Annals of Hepatology 27 (2022) 100678

Contents lists available at ScienceDirect

Annals of Hepatology

journal homepage: www.elsevier.es/annalsofhepatology

Original article

Circ-LARP1B knockdown restrains the tumorigenicity and enhances radiosensitivity by regulating miR-578/IGF1R axis in hepatocellular carcinoma

Shuangmei Zhu, Yong Chen, Hong Ye, Baoqiang Wang, Xiang Lan, Hanying Wang, Sijie Ding, Xiao He*

Department of Radiation Oncology, Lishui People's Hospital, No.15 Dazhong Street, Liandu District, Lishui, Zhejiang 323000, China

ARTICLE INFO

Article History:
Received 5 December 2021
Accepted 17 January 2022
Available online 27 January 2022

Keywords:
circ-LARP1B
miR-578
IGF1R
Radiosensitivity
Hepatocellular carcinoma
Tumorigenesis

ABSTRACT

Introduction and Objectives: Circular RNA La Ribonucleoprotein 1B (circ-LARP1B) was reported to serve as an oncogene in many types of cancers. Radiotherapy (RT) is an important element of the multimodal treatment concept in malignancies. Here, this work aimed to investigate the role of circ-LARP1B in the tumorigenesis and radiosensitivity of hepatocellular carcinoma (HCC).

Patients or Materials and Methods: Quantitative real-time polymerase chain reaction (qRT-PCR) and Western blot were used to detect the expression of genes and proteins. *In vitro* experiments were conducted using cell counting Kit-8 (CCK-8), colony formation, EDU, transwell, and tube formation assays, respectively. Dual-luciferase reporter assay was employed to identify the target relationship between miR-578 and circ-LARP1B or IGF1R (insulin-like growth factor 1 receptor). *In vivo* assay was performed using murine xenograft model.

Results: Circ-LARP1B was highly expressed in HCC tissues and cells, and high expression of circ-LARP1B was closely associated with poor prognosis. Functional experiments demonstrated that circ-LARP1B silencing impaired cell proliferation, invasion, angiogenesis and reduced radioresistance *in vitro*. Mechanistically, circ-LARP1B could competitively bind with miR-578 to relieve the repression of miR-578 on the expression of its target gene IGF1R. Further rescue assay confirmed that miR-578 inhibition reversed the inhibitory effects of circ-LARP1B knockdown on HCC cell malignant phenotypes and radioresistance. Moreover, miR-578 overexpression restrained tumorigenicity and enhanced radiosensitivity in HCC cells, which were attenuated by IGF1R up-regulation. Besides that, circ-LARP1B knockdown impeded tumor growth and enhanced irradiation sensitivity in HCC *in vivo*.

Conclusions: Circ-LARP1B knockdown restrained HCC tumorigenicity and enhanced radiosensitivity by regulating miR-578/IGF1R axis, providing a new target for the treatment of HCC.

1. Introduction

Hepatocellular carcinoma (HCC) is one of the most common malignancies all over the world with high morbidity, mortality and recurrence rate [1,2]. Currently, surgical interventions are the only chance for achieving cure in HCC patients, however, the majority of patients present in an unresectable advanced stage [3]. Although a number of drugs, such as combination therapies and immune checkpoint inhibitors, have been developed [4–6], overall survival of patients with advanced disease remains poor. Radiotherapy (RT) is an important element of the multimodal treatment concept, commonly used for both curative and palliative therapies of many types of malignancies [7]. Radiotherapy, such as stereotactic body radiotherapy (SBRT) and radiofrequency ablation (RFA), has emerged as an effective locally ablative therapy in treating unresectable HCC [8,9]. Thus, further clarification on the molecular mechanisms involving tumorigenesis and radiosensitivity in HCC is imperative.

Circular RNAs (circRNAs) are a kind of evolutionarily conserved RNA molecules lacking the 3' and 5' ends [10]. They are abundant in eukaryotes, and often exhibit development- or tissue-specific expression pattern [11]. Moreover, accumulating evidence has reported

Abbreviations: circ-LARP1B, Circular RNA La Ribonucleoprotein 1B; HCC, hepatocellular carcinoma; CCK-8, cell counting Kit-8; qRT-PCR, Quantitative real-time polymerase chain reaction; RT, Radiotherapy; RFA, radiofrequency ablation; SBRT, stereotactic body radiotherapy; FBS, Fetal bovine serum; NC, negative control; GAPDH, glyceraldehyde-3-phosphate dehydrogenase; FCM, Flow cytometry; FITC, fluorescein isothiocyanate; PI, propidium iodide; TCM, tumor-conditioned medium; PVDF, polyvinylidene fluoride; MMP9, matrix metallopeptidase; ECL, enhanced chemiluminescence system; WT, wild-type

* Corresponding author.
E-mail address: hexiao1503@163.com (X. He).

https://doi.org/10.1016/j.aohep.2022.100678

that circRNAs are implicated in a broad range of cell biological processes related to carcinogenesis, metastasis, and apoptosis, implying the potential role of circRNAs in cancer diagnosis and therapy [12–15]. For example, hsa_circ_0008274 overexpression could inhibit the proliferation and invasion of lung adenocarcinoma cells via up-regulating HMGA2 through sequestering miR-578 [16]. CircRNA_0000285 facilitated the growth and metastasis of cervical cancer by elevating FUS [17]. Circ-LARP1B (ID: hsa_circ_0070934) is a functional circRNA derived from the LARP1B (La Ribonucleoprotein 1B) gene, and has been demonstrated to be overexpressed in cutaneous squamous cell carcinoma, which is beneficial to cell invasive and proliferative abilities [18,19]. However, the functions of circ-LARP1B in HCC remain largely undefined.

Hence, the purpose of this work was to investigate the action of circ-LARP1B in HCC tumorigenicity and radiosensitivity. Moreover, we also explored the action mode of circ-LARP1B in regulating HCC progression, which may provide a novel therapeutic target for HCC.

2. Materials and methods

2.1. Clinical tissue specimens

Thirty-nine cases of HCC patients newly diagnosed by pathological examination at XXXXXX were included in this study. HCC tissues and matched non-cancer tissues were collected by surgery, and embedded in paraffin for further immunohistochemical (IHC) analysis with Ki67 (ab16667, Abcam, Cambridge, MA, USA) as described previously [20]. For tissue morphology analysis, the hematoxylin and eosin (H&E) staining was conducted. All samples were stored at -80 ° C until used. All subjects had provided written informed consent, and this work was approved by the Ethics Committee of XXXXXX.

2.2. Cell culture

Human HCC cell lines (MHCC97, Hep3B and Huh-7) and human normal liver epithelial cells (THLE-2) were provided by Biotechnology (Shanghai, China), and grown in 5% CO_2 at 37°C with Dulbecco's Modified Eagle's Medium (DMEM; Life Technologies, Scotland, UK) plus 1% penicillin/streptomycin (Invitrogen, Camarillo, CA, USA) and 10% fetal bovine serum (FBS) (Life Technologies).

2.3. Plasmid transfection

The designed shRNAs for circ-LARP1B (sh-circ-LARP1B) and nontarget shRNA (sh-NC), miR-578 mimic or inhibitor (miR-578 or anti-miR-578) and the negative control (NC) were procured from Genechem (Shanghai, China). The pCD5-ciR/circ-LARP1B (circ-LARP1B) or pcDNA3.1/IGF1R (IGF1R) overexpression plasmids were constructed via cloning corresponding cDNA into pCD5-ciR or pcDNA3.1 vectors (Invitrogen, Carlsbad, CA, USA) to overexpress circ-LARP1B or IGF1R, with empty pCD5-ciR or pcDNA3.1 as NC (pCD5-ciR or pcDNA). Then Hep3B and Huh-7 cells were transiently transfected with 100 nM of shRNA, 100 ng of plasmid, or 50 nM of miRNA mimic or inhibitor using Lipofectamine 3000 (Invitrogen). Besides, lentivirus plasmids of sh-circ-LARP1B and sh-NC were synthesized at HanBio (Shanghai, China) for animal experiments.

2.4. Quantitative real-time PCR (qRT-PCR)

Total RNA was prepared as per the protocol of RNeasy Mini Kit (Qiagen, Crawley, UK). The PARIS Kit (Life Technologies, USA) was employed to conduct the separation of nuclear and cytoplasmic RNAs. For circRNA detection, treatment with RNase R (3 U/mg, Geneseed, Guangzhou, China) in total RNAs (5 μg) from cells was implemented at 37 °C for 15 min. Then isolated RNAs (2 ug) were reverse-transcribed into cDNA using a cDNA synthesis kit (Takara, Shiga, Japan), and quantitative PCR was performed with SYBR QPCR Mix (Takara) to monitor the gene expression. The relative expression was processed by the $2^{-\Delta\Delta Ct}$ method and normalized to glyceraldehyde-3-phosphate dehydrogenase (GAPDH) or U6. The primer sequences were listed:

circ-LARP1B: F 5'-CCGAGGTTCCTTTAGAGGTCG-3', R 5'- GACGCTCTGAAATCCAGTGT-3';
LARP1B: F 5'-GCCAACACCAAGTGAATTAGTGA-3', R 5'-TTTGTTTCCCGGTTTTCTTTGC-3';
IGF1R: F 5'-AGGATATTGGGCTTTACAACCTG-3', R 5'- GAGGTAACAGAGGTCAGCATTTT-3'.
GAPDH: F 5'-CCCACATGGCCTCCAAGGAGTA-3', R 5'-GTGTACATGGCAACTGTGAGGAGG-3';
miR-578: F 5'-GCCGAGCTTCTTGTGCTCTAG-3', R 5'-GCGAGCA CAGTG CAGGGTCCGAGGTAT-3';
U6: F 5'-CTCGCTTCGGCAGCACA-3', R 5'-AACGCTTCACGAATTTGCGT-3'.

2.5. Cell counting Kit-8 (CCK-8) assay

At the culture of 0, 24, 48, or 72 h, 10 μL of CCK-8 (5 mg/mL) (Solarbio, Beijing, China) was added into each well with transfected Hep3B and Huh-7 cells (10000 cells/well) and then incubated for another 2 h. The proliferation curves were determined by reading absorbance at 490 nm.

2.6. Colony formation assay

Clonogenic transfected Hep3B and Huh-7 cells were prepared for two week in 6-well plates with 1000 cells/well. After being fixed with methanol, cell colonies were stained with 1% crystal violet (Solarbio), followed by visualizing and counting manually.

2.7. 5-ethynyl-2'-deoxyuridine (EDU) assay

Transfected Hep3B and Huh-7 cells were seeded onto a 96-well plate (2×10^4 cells/well) embracing EDU medium diluent (RiboBio, Guangzhou, China) and incubated for 3 h. After being fixed and permeabilized, cells were incubated with Apollo reaction mixture under darkness for 30 min. Cell nuclei were stained by DAPI. The EDU positive cells were visualized using a fluorescence microscope to evaluate cell proliferation.

2.8. Flow cytometry (FCM) assay

After transfection, Hep3B and Huh-7 cells were harvested by trypsinization, followed by resuspending in binding buffer (1 ×). Then cells were stained orderly with Annexin V-fluorescein isothiocyanate (FITC) (Life Technologies) and propidium iodide (PI) (Abcam). The apoptotic cells were then determined using a FACScan flow cytometry (BD Biosciences, Franklin Lakes, NJ, USA).

2.9. Transwell assay

Transwell inserts in 24-wells (Costar, Corning, Switzerland) with Matrigel-coated membrane (BD Biosciences) were used for cell invasion analysis. Transfected Hep3B and Huh-7 cells with 200 μL serum-free DMEM were seeded into the upper chambers, and 600 μL of complete culture medium was filled into the lower chamber. 24 h later, the invaded cells were imaged and counted using a microscope after being fixed and stained with 0.1% crystal violet solution (Solarbio).

2.10. Tube formation assay

After transfection, Hep3B and Huh-7 cells were grown in serum-free DMEM for 48 h to obtain tumor-conditioned medium (TCM). The wells of a 48-well plate were coated with 75 μL of Matrigel and solidified for more than 1 h at 37 °C. Then HUVECs (Biotechnology) with TCM were seeded onto the gel and incubated for another 6 h. A microscope was used to observe and quantify the tube formation of HUVECs and acquire images.

2.11. Survival fraction analysis

Transfected Hep3B and Huh-7 cells were seeded into a 6-well plate after 48 h of transfection and irradiated with 0, 2, 4, 6 or 8 Gy for 48 h. After incubation for 14 days at 37 °C, cell colonies were fixed with methanol and stained with 1% crystal violet (Solarbio), and colonies with more than 50 cells were selected and counted to calculate survival fraction according to the formula (number of colonies/number of cells plated) $_{\text{irradiated}}$/(number of colonies/number of cells plated)$_{\text{non-irradiated}}$.

2.12. Western blot

Total isolated proteins were separated by 10% polyacrylamide gel and then transferred onto a polyvinylidene fluoride (PVDF) membrane (Millipore, Darmstadt, Germany). The membrane was interacted with indicated primary antibodies all night at 4°C, followed by incubation with a goat anti-rabbit or anti-mouse-HRP-conjugated secondary antibody (ab6721 and ab6789, 1:5000, Abcam). The protein bands were studied using the enhanced chemiluminescence system (ECL; Solarbio). The primary antibodies included anti-B-cell lymphoma-2 (anti-Bcl-2) (1:1000, ab194583), anti-matrix metallopeptidase 9 (MMP9) (1:2000, ab38898), anti-IGF1R (1:2000, ab39398) and anti-GAPDH (1:5000, ab181602), all obtained from Abcam.

2.13. Dual-luciferase reporter assay

Circ-LARP1B or IGF1R 3'UTR fragments covering wild-type (WT) and mutated (MUT) miR-578 binding sites were amplified and inserted into the PGL3 Basic vector (Invitrogen). Then Hep3B and Huh-7 cells were co-transfected with 50 ng PGL3 vector, 10 ng pRL-TK Renilla vector and 50 nM miR-578 mimic or mimic NC, respectively. Then luciferase activity was analyzed with the Renilla activity as normalization.

2.14. Tumor xenograft assay

This study was conducted strictly in line with the guidelines of Animal Care and Use Committee of XXXXXX. Six-weeks-old BALB/c nude mice were purchased from Charles River Labs (Beijing, China) and randomly divided into four group (N = 7 per group). Huh-7 cells (4×10^6/0.2 mL PBS), infected with lentiviral plasmids mediated of sh-circ-LARP1B or sh-NC, were subcutaneously injected into the right flank of blindly randomized nude mice, respectively. When xenograft

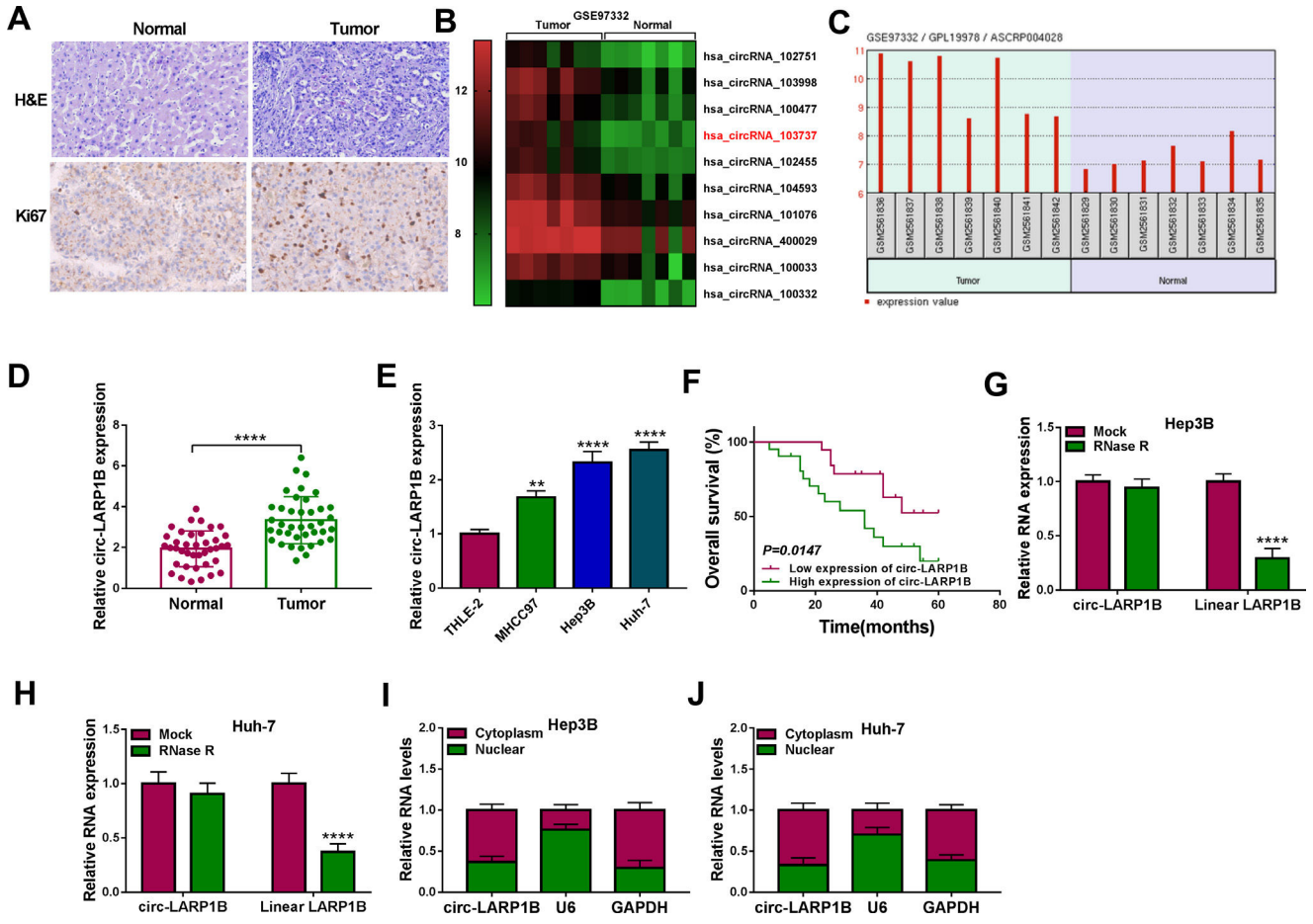

Fig. 1. Circ-LARP1B is highly expressed in HCC tissues and cells. (A) Heat maps showing the 10 up-regulated circRNAs between 7 paired HCC tissues and normal tissues (GSE91332). Red represents high expression and green represents low expression. (B) Circ-LARP1B expression was higher in HCC tissues compared with paired normal tissues. (C) Representative images of H&E and Ki67 staining in HCC tissues and normal tissues. (D, E) qRT-PCR analysis of circ-LARP1B level in HCC tissues and adjacent normal tissues, as well as in HCC cells and normal THLE-2 cells. (F) The Kaplan-Meier curve analyzed showed the association between circ-LARP1B expression and overall survival of HCC patients (n = 39). (G, H) qRT-PCR analysis of circ-LARP1B expression in Hep3B and Huh-7 cells treated with or without RNase R. (I, J) qRT-PCR indicating the distribution of circ-LARP1B in the cytoplasmic and nuclear fractions of Hep3B and Huh-7 cells. $^{**}P$<0.01, $^{****}P$<0.0001.

reached to 60 mm^3, mice of two groups were treated with 6 Gy. Tumor size was measured every 4 days with a Vernier caliper, and tumor volume was calculated as volume = (length × width2)/2. At day 28, mice were sacrificed, the tumors were excised, weighed and divided either for the detection of circ-LARP1B, miR-578 and IGF1R by qRT-PCR and Western blot, or fixed in formalin for IHC analysis.

2.15. Statistical analysis

Data were presented as mean ± standard deviation. Statistical analyses were conducted using paired, unpaired t test, Mann-Whitney test or analysis of variance. The expression correlation was analyzed using Pearson's correlation coefficient assay. The survival curve of patients was determined by the Kaplan-Meier method and log-rank test. $P < 0.05$ suggested significant differences. ($^{*}P < 0.05$, $^{**}P < 0.01$, $^{***}P < 0.001$, $^{****}P < 0.0001$)

3. Results

3.1. Circ-LARP1B is highly expressed in HCC tissues and cells, and associated with poor outcomes in HCC patients

CircRNA microarray was conducted to screen the differentially expressed circRNAs in HCC. Data mining of GEO (http://www.ncbi.nlm.nih.gov/geo) datasets (GSE91332) showed the top 10 up-regulated circRNAs (log2|fold change| ≥ 2 and $P < 0.05$) (Fig. 1A). Among them, we noted that the expression of a circRNA (circ-LARP1B, ID: hsa_circRNA_103737) labeled as ASCRP004028 was obviously raised in HCC tissues (Fig. 1B). Therefore, we particularly focused on this uncharacterized circRNA for further evaluation. A total of 39 pairs of HCC tissues and adjacent normal tissues were collected from HCC patients. The representative HE staining was shown in Fig. 1C. Moreover, IHC analysis confirmed that Ki67 expression was increased in HCC tissues compared with normal tissues (Fig. 1C). Thereafter, the expression of circ-LARP1B in clinical tissues was investigated. The qRT-PCR analysis showed that circ-LARP1B expression was higher in HCC tissues than those in normal liver tissues (Fig. 1D). Similarly, we also observed a high expression of circ-LARP1B in HCC cells (MHCC97, Hep3B and Huh-7) compared with liver epithelial cell THLE-2 (Fig. 1E). Additionally, the survival curve was established to assess the prognostic value of circ-LARP1B, which showed that high circ-LARP1B level was associated with a shorter overall survival time (Fig. 1F). Subsequently, the stability of circ-LARP1B was investigated, circ-LARP1B was significantly resistant to efficient RNase R digestion compared with linear LARP1B in Hep3B and Huh-7 cells (Fig. 1G, H). Besides, we also found that circ-LARP1B was mainly located in the cytoplasm in Hep3B and Huh-7 cells (Fig. 1I, J). Collectively, these data suggested that circ-LARP1B was elevated in HCC and high expression of circ-LARP1B was associated with poor outcomes in HCC patients.

3.2. Knockdown of circ-LARP1B suppresses tumorigenesis and enhances radiosensitivity in HCC cells

To investigate the functions of circ-LARP1B in tumorigenesis and radiosensitivity in HCC, the shRNAs targeting circ-LARP1B were established and stably transfected into Hep3B and Huh-7 cells, resulting in its knockdown (Fig. 2A). Silencing of circ-LARP1B decreased the proliferation (Fig. 2B, C), colony-formation abilities (Fig. 2D), and DNA synthesis activities (Fig. 2E) in Hep3B and Huh-7 cells. Conversely, circ-LARP1B knockdown led to an increase of the apoptosis rate of Hep3B and Huh-7 cells (Fig. 2F). The invasion ability of circ-LARP1B-repressed Hep3B and Huh-7 cells was significantly reduced (Fig. 2G). Besides that, circ-LARP1B knockdown induced HUVECs to develop fewer and smaller tubes (Fig. 2H). After that, we investigated the role of circ-LARP1B in irradiation sensitivity in HCC cells. Transfected Hep3B and Huh-7 cells were treated with different doses of irradiation (0, 2, 4, 6 or 8 Gy), which manifested that circ-LARP1B knockdown remarkably decreased cell survival fraction with the increase of radiotherapy dose (Fig. 2I, J). In addition, the apoptosis- and invasion-related markers were detected, Western blot analysis showed that circ-LARP1B silencing down-regulated the protein levels of Bcl-2 and MMP9 in Hep3B and Huh-7 cells (Fig. 2K, L), further implying the inhibition of cell apoptosis and invasion. Taken together, knockdown of circ-LARP1B suppressed the malignant behaviors and enhanced radiosensitivity in HCC cells *in vitro*.

3.3. MiR-578 is a target of circ-LARP1B in HCC cells

Subcellular fractionation assay showed that circ-LARP1B mainly amassed in the cytoplasm of HCC cells, suggesting the potential of circ-LARP1B serving as a miRNA sponge. Through the prediction of circinteractome database, miR-578 was found to have the complementary sequences in circ-LARP1B (Fig. 3A). To validate the interaction between miR-578 and circ-LARP1B, the elevation efficiency of miR-578 mimic was firstly confirmed using qRT-PCR (Fig. 3B). After that, results of dual-luciferase reporter assay showed that augmented expression of miR-578 significantly reduced the luciferase activity of WT-circ-LARP1B but not the MUT-circ-LARP1B in Hep3B and Huh-7 cells (Fig. 3C, D), indicating the binding between miR-578 and circ-LARP1B. Subsequently, we found that miR-578 expression was decreased in HCC tissues (Fig. 3E), which was negatively correlated with circ-LARP1B expression (Fig. 3F). Also, its expression was lower in Hep3B and Huh-7 cells than those of THLE-2 cells (Fig. 3G). Importantly, after validating the transfection efficiency of circ-LARP1B overexpressing vector (Fig. 3H), it was observed that miR-578 expression was decreased by circ-LARP1B overexpression but increased by circ-LARP1B down-regulation in Hep3B and Huh-7 cells (Fig. 3I). In conclusion, circ-LARP1B directly targeted miR-578 and repressed its expression in HCC cells.

3.4. Circ-LARP1B silencing suppresses tumorigenesis and enhances radiosensitivity in HCC cells via miR-578

Next, we elucidated whether miR-578 was a functional gene for circ-LARP1B by performing rescue experiments. MiR-578 inhibitor was transfected into circ-LARP1B-decraesed Hep3B and Huh-7 cells, as expected, miR-578 inhibitor decreased circ-LARP1B knockdown-induced elevation of miR-578 in cells (Fig. 4A). Then results of a series of rescue experiments exhibited that miR-578 inhibitor abolished circ-LARP1B knockdown-evoked suppression of cell proliferation (Fig. 4B-E), enhancement of cell apoptosis (Fig. 4F), and impairment of cell invasion in Hep3B and Huh-7 cells (Fig. 4G). Moreover, the falling trend of HUVEC tube formation ability (Fig. 4H) and the promotion of Hep3B and Huh-7 cell radiosensitivity (Fig. 4I, J) imposed by circ-LARP1B knockdown were attenuated in response to the inhibition of miR-578. Western blot analysis displayed that miR-578 inhibitor led to the increase of Bcl-2 and MMP9 protein levels in circ-LARP1B-repressed Hep3B and Huh-7 cells (Fig. 4K, L). Collectively, circ-LARP1B regulated HCC tumorigenesis and radiosensitivity by miR-578.

3.5. IGF1R is a target of miR-578 in HCC cell

It has been documented that miRNAs can regulate the expression of target genes via binding to their 3'UTR. Through the use of starBase v2.0 database, IGF1R was a putative mRNA that could be recognized by miR-578 (Fig. 5A). Dual-luciferase reporter assay certified that overexpression of miR-578 significantly declined the luciferase activity of the IGF1R 3'UTR-WT vector but failed to decrease that of the mutant vector (Fig. 5B, C). IGF1R mRNA expression was discovered to

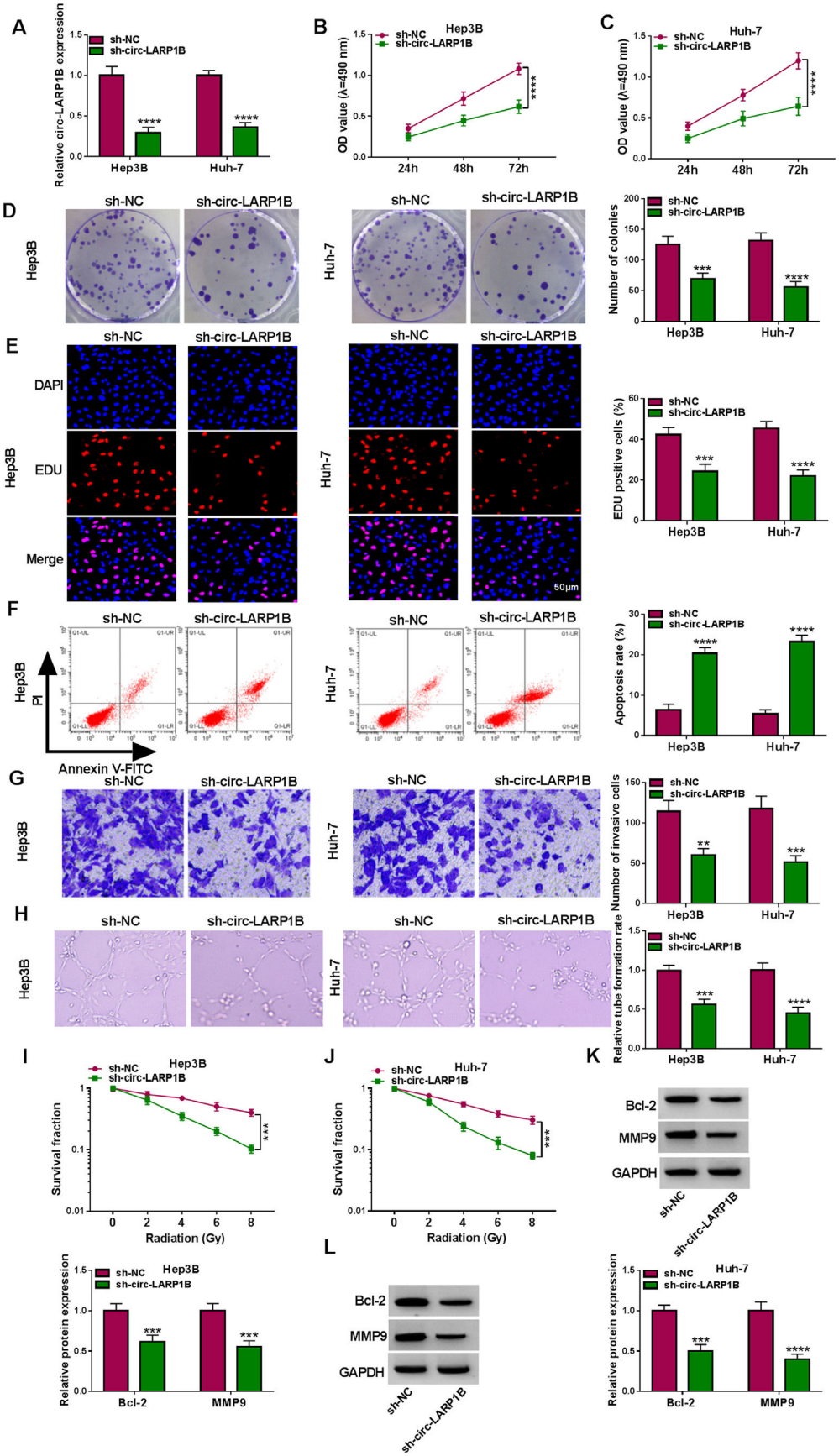

Fig. 2. Knockdown of circ-LARP1B suppresses tumorigenesis and enhances radiosensitivity in HCC cells. (A-L) Hep3B and Huh-7 cells were transfected with sh-NC or sh-circ-LARP1B. (A) Detection of circ-LARP1B expression in cells using qRT-PCR. (B-E) Cell proliferation analysis using CCK-8, colony formation, and EDU assays. (F) Cell apoptosis analysis using FCM. (G) Transwell assay for cell invasion. (H) Tube formation ability of HUVECs cultivated in the TCM from transfected cells. (I, J) Colony formation assay for survival fraction in cells exposed to various doses of irradiation (0, 2, 4, 6 or 8 Gy). (K, L) Western blot analysis for the levels of Bcl-2 and MMP9 protein. $^{**}P<0.01$, $^{***}P<0.001$, $^{****}P<0.0001$.

be increased in HCC tissues (Fig. 5D), which negatively correlated with miR-578 expression (Fig. 5E). Besides that, the protein level of IGF1R in HCC tissues and cells was also elevated (Fig. 5F,G). Moreover, it was proved that miR-578 up-regulation or down-regulation markedly decreased or increased IGF1R expression in Hep3B and Huh-7 cells (Fig. 5H). These results confirmed that miR-578 targeted IGF1R and negatively regulated its expression.

3.6. MiR-578 suppresses tumorigenesis and enhances radiosensitivity in HCC cells via IGF1R

Furthermore, we designed and performed rescue assays to demonstrate the regulatory role of miR-578/IGF1R axis in HCC. Hep3B and Huh-7 cells were co-transfected with miR-578 mimic and IGF1R overexpressing vector, and the transfection efficiencies were then validated by Western blot (Fig. 6A). As expected, miR-578 overexpression reduced the proliferation rate (Fig. 6B-E) and increased the apoptosis rate (Fig. 6F) in Hep3B and Huh-7 cells, which were reversed by IGF1R up-regulation (Fig. 6B-F). Transwell assay showed that miR-578 up-regulation suppressed cell invasion, while co-transfection with IGF1R in Hep3B and Huh-7 cells exhibited opposite trend (Fig. 6G). The descending tube formation ability in HUVECs induced by miR-578 up-regulation was restored by IGF1R (Fig. 6H). Besides, the enhancement on radiosensitivity (Fig. 6I, J) and decreased Bcl-2 and MMP9 expression (Fig. 6K, L) caused by miR-578 up-regulation were also both counteracted by IGF1R overexpression. Altogether, miR-578 targeted IGF1R to regulate HCC cell tumorigenesis and radiosensitivity.

3.7. Circ-LARP1B can regulate IGF1R expression through miR-578

Thereafter, we probed the circ-LARP1B/miR-578/IGF1R axis in HCC cells. As shown in Fig. 7A, B, knockdown of circ-LARP1B led to a decrease of IGF1R expression both at mRNA and protein levels, which was rescued by the inhibition of miR-578 in Hep3B and Huh-7 cells, implying the feedback loop of circ-LARP1B/miR-578/IGF1R in HCC.

3.8. Circ-LARP1B silencing impedes tumor growth, migration and enhances irradiation sensitivity in HCC in vivo

Additionally, to explore the effects of circ-LARP1B on HCC tumorigenesis and radiosensitivity, we also performed *in vivo* assay using a mouse model. Circ-LARP1B silencing or irradiation treatment reduced tumor volume and weight, moreover, circ-LARP1B knockdown combined with irradiation led to a greater inhibition on tumor growth (Fig. 8A, B). Furthermore, as exhibited in Fig. 8C, D, circ-LARP1B knockdown caused the decrease of circ-LARP1B and IGF1R expression levels and increase of miR-578 expression in tumors from

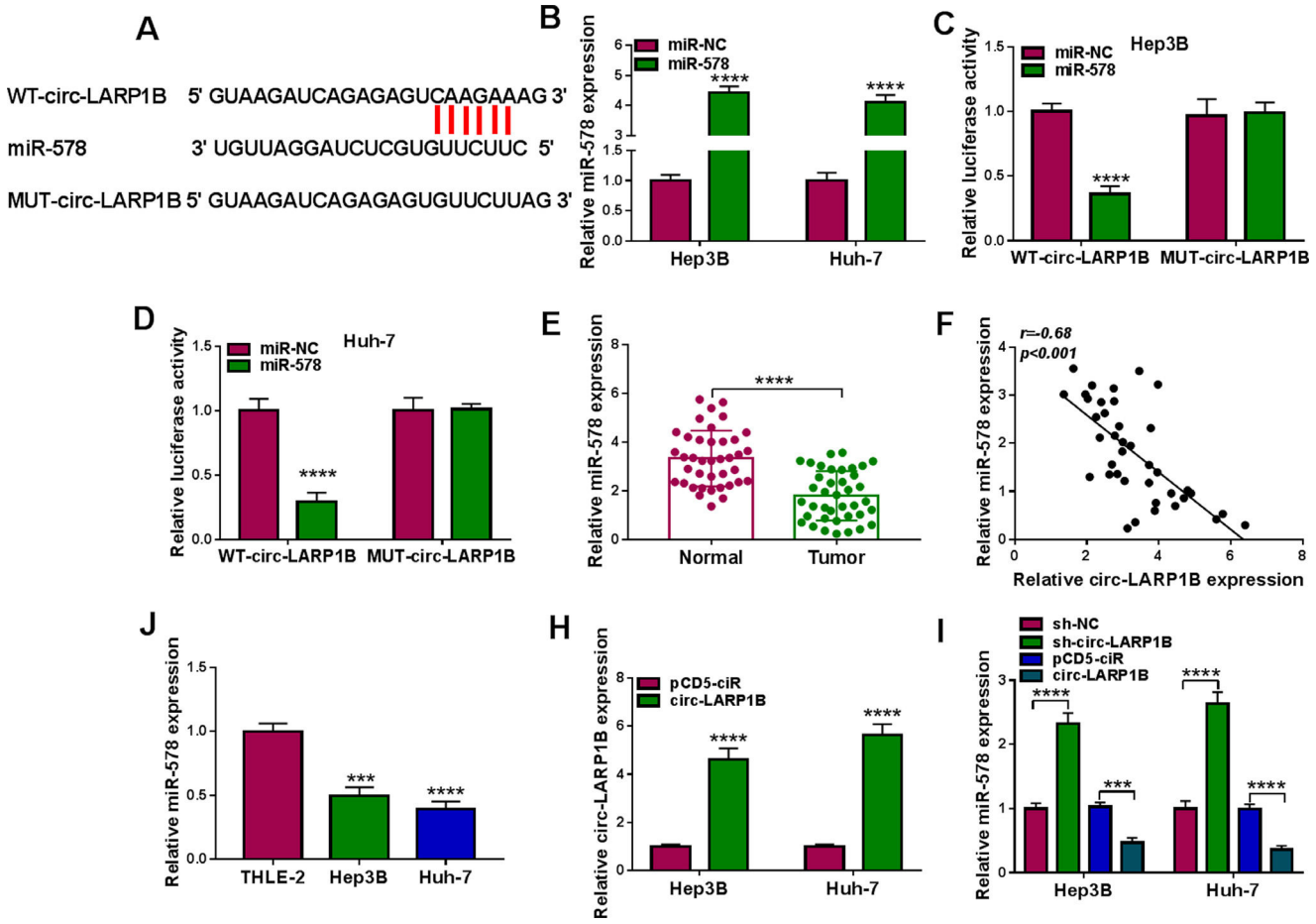

Fig. 3. MiR-578 is a target of circ-LARP1B in HCC cells. (A) The potential binding sites between circ-LARP1B and miR-578. (B) qRT-PCR analysis of miR-578 expression in Hep3B and Huh-7 cells transfected with miR-578 mimic or mimic NC (miR-NC). (C, D) Dual-luciferase reporter assay for the luciferase activity of wild-type and mutated circ-LARP1B reporter after miR-578 overexpression in Hep3B and Huh-7 cells. (E) qRT-PCR analysis of miR-578 level in HCC tissues and adjacent normal tissues. (F) Pearson's correlation coefficient analysis for the correlation between miR-578 and circ-LARP1B expression in HCC tissues. (J) qRT-PCR analysis of miR-578 level in HCC cells and normal THLE-2 cells. (H) qRT-PCR analysis of circ-LARP1B expression in Hep3B and Huh-7 cells transfected with pCD5-ciR or circ-LARP1B. (I) qRT-PCR analysis of miR-578 expression in Hep3B and Huh-7 cells transfected with pCD5-ciR, circ-LARP1B, sh-NC or sh-circ-LARP1B. ***P<0.001, ****P<0.0001.

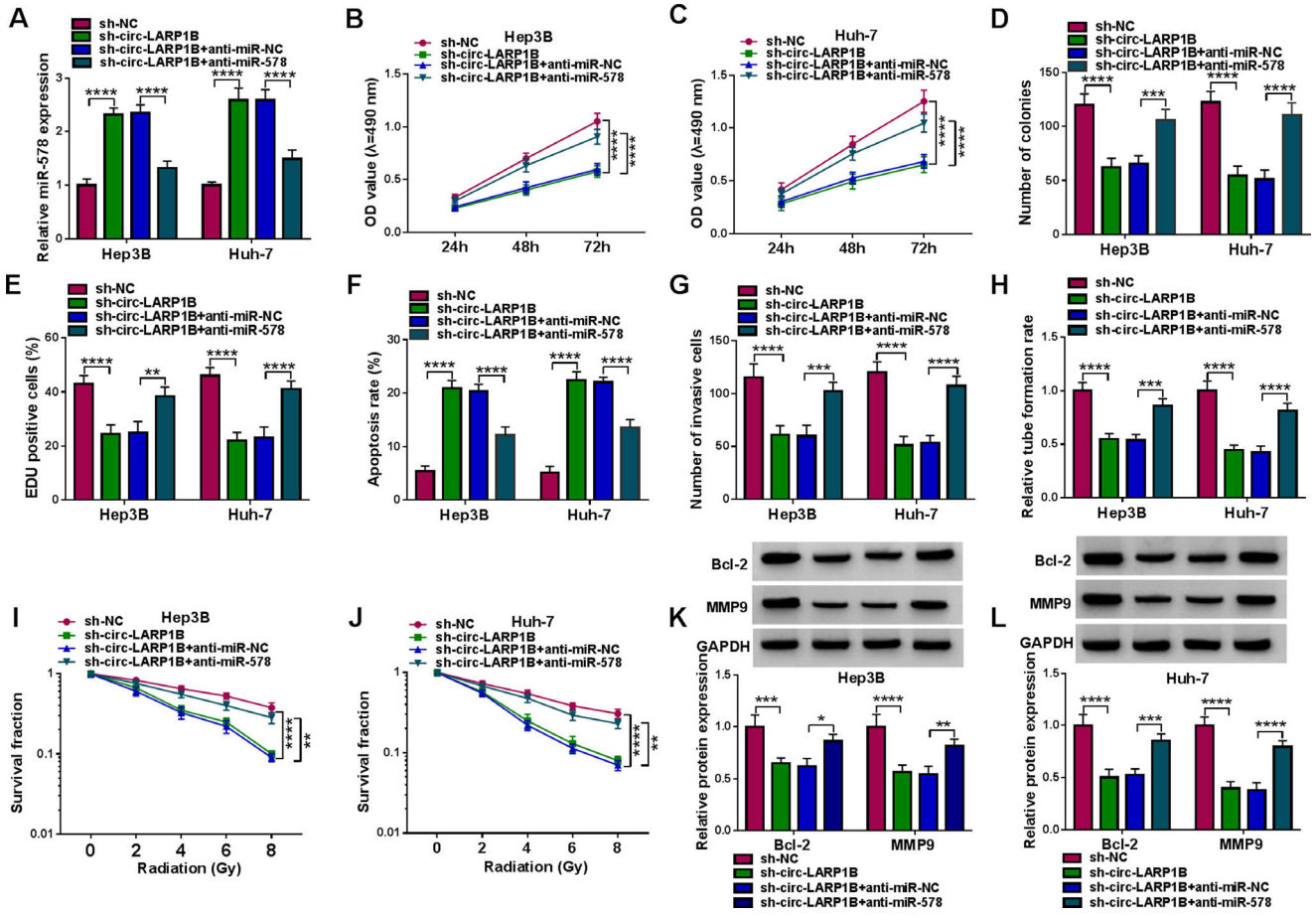

Fig. 4. Circ-LARP1B silencing suppresses tumorigenesis and enhances radiosensitivity in HCC cells via miR-578. (A-L) Hep3B and Huh-7 cells were transfected with sh-NC, sh-circ-LARP1B, sh-circ-LARP1B + anti-miR-NC, sh-circ-LARP1B + anti-miR-578. (A) Detection of miR-578 expression in cells using qRT-PCR. (B-E) Cell proliferation analysis using CCK-8, colony formation, and EDU assays. (F) Cell apoptosis analysis using FCM. (G) Transwell assay for cell invasion. (H) Tube formation ability of HUVECs cultivated in the TCM from transfected cells. (I, J) Colony formation assay for survival fraction in cells exposed to various doses of irradiation (0, 2, 4, 6 or 8 Gy). (K, L) Western blot analysis for the levels of Bcl-2 and MMP9 protein. $^{*}P<0.05$, $^{**}P<0.01$, $^{***}P<0.001$, $^{****}P<0.0001$.

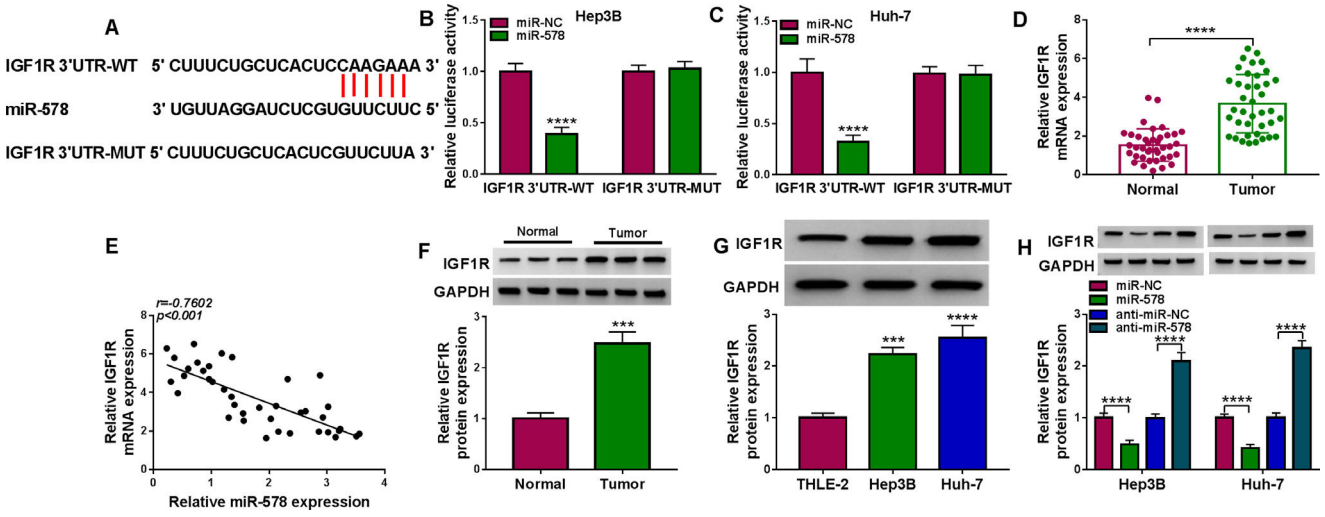

Fig. 5. IGF1R is a target of miR-578 in HCC cell. (A) The potential binding sites between IGF1R and miR-578. (B, C) Dual-luciferase reporter assay for the luciferase activity of wild-type and mutated IGF1R reporter after miR-578 overexpression in Hep3B and Huh-7 cells. (D) qRT-PCR analysis of IGF1R mRNA in HCC tissues and adjacent normal tissues. (E) Pearson's correlation coefficient analysis for the correlation between miR-578 and IGF1R expression in HCC tissues. (F, G) Western blot analysis of IGF1R protein level in HCC tissues and adjacent normal tissues, as well as in HCC cells and normal THLE-2 cells. (H) Western blot analysis of IGF1R expression in Hep3B and Huh-7 cells transfected with miR-578, miR-NC, anti-miR-578, or anti-miR-NC. $^{***}P<0.001$, $^{****}P<0.0001$.

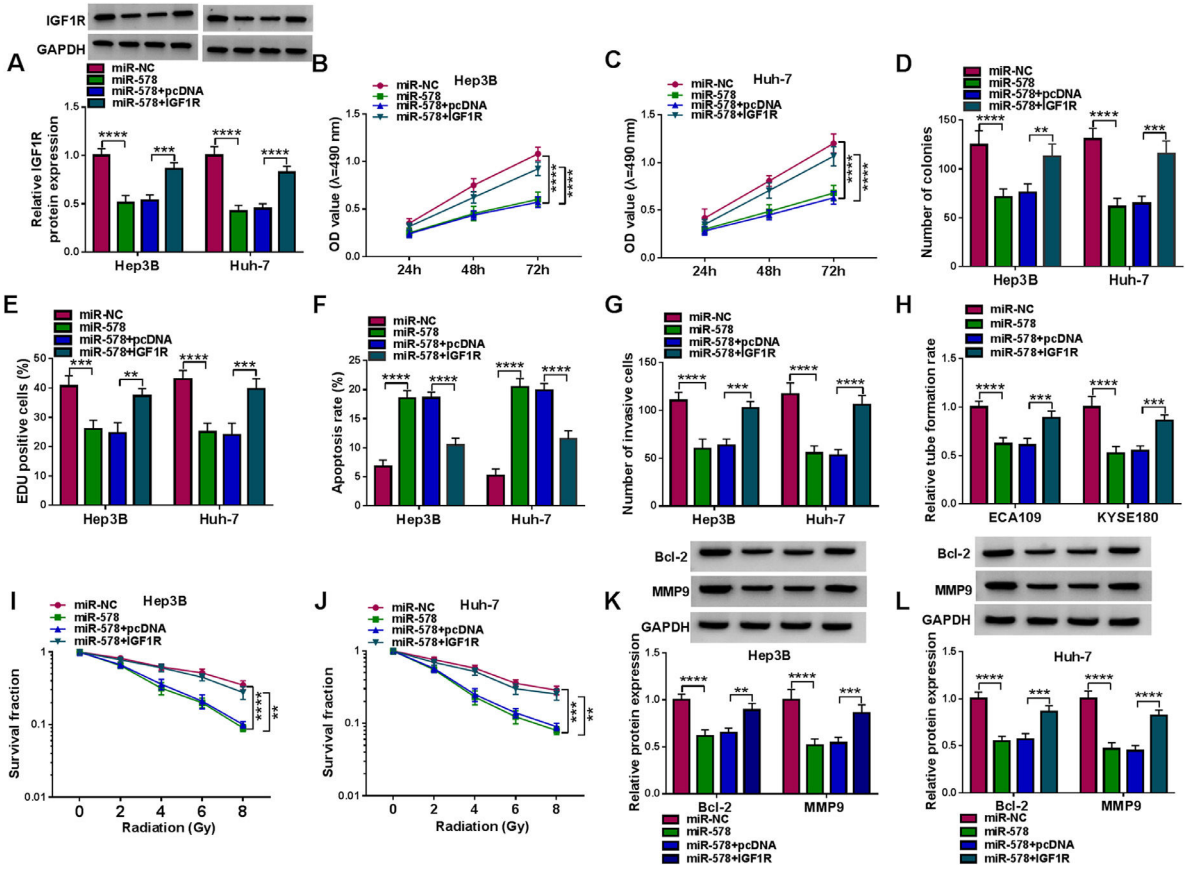

Fig. 6. MiR-578 suppresses tumorigenesis and enhances radiosensitivity in HCC cells via IGF1R. (A-L) Hep3B and Huh-7 cells were co-transfected with miR-NC, miR-578, miR-578 + pcDNA, or miR-578 + IGF1R. (A) Detection of IGF1R expression in cells using Western blot. (B-E) Cell proliferation analysis using CCK-8, colony formation, and EDU assays. (F) Cell apoptosis analysis using FCM. (G) Transwell assay for cell invasion. (H) Tube formation ability of HUVECs cultivated in the TCM from transfected cells. (I, J) Colony formation assay for survival fraction in cells exposed to various doses of irradiation (0, 2, 4, 6 or 8 Gy). (K, L) Western blot analysis for the levels of Bcl-2 and MMP9 protein. $^{**}P<0.01$, $^{***}P<0.001$, $^{****}P<0.0001$.

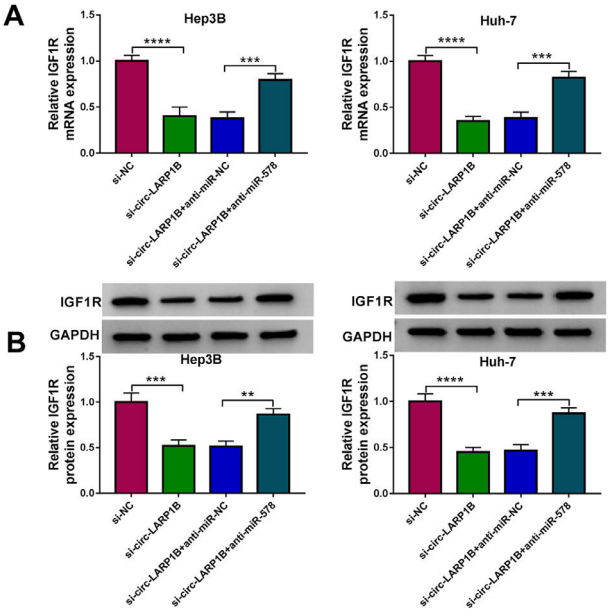

Fig. 7. Circ-LARP1B can regulate IGF1R expression through miR-578. (A, B) qRT-PCR and Western blot analysis of IGF1R expression in Hep3B and Huh-7 cells transfected with sh-NC, sh-circ-LARP1B, sh-circ-LARP1B + anti-miR-NC, sh-circ-LARP1B + anti-miR-578. $^{**}P<0.01$, $^{***}P<0.001$, $^{****}P<0.0001$.

circ-LARP1B-dwon-regulated group with or without irradiation treatment. Besides that, IHC staining showed that deletion of circ-LARP1B or irradiation treatment alone, or the combination of them also caused the decrease of IGF1R, Bcl-2 and MMP9 in xenograft tumors (Fig. 8E). In a word, circ-LARP1B suppressed tumor growth, migration and enhanced irradiation sensitivity in HCC *in vivo* by regulating miR-578/IGF1R axis.

4. Discussion

Globally, HCC is the second cancer-related death carrying a 5-year overall survival (OS) rate of around 5% [21]. RT is one of the main treatment modalities, and is utilized either alone or more commonly in combination with chemotherapy and surgery in more than 50% of all malignancies [22]. It can result in the break of DNA double-stranded through direct DNA ionization or indirect stimulation of reactive oxygen species [23], benefiting in controlling the local recurrence and improving the tumor prognosis [7,24]. Therefore, enhancing the radiosensitivity of cancer cells may be a promising therapeutic strategy for improving the outcome of HCC patients.

Recently, circRNAs have increasingly attracted great research interest in the field of cancer research. CircRNAs have been reported to be differentially expressed in various malignancies and deregulation of circRNAs participate in the progression and drug resistance in many types of cancers, including HCC [25,26]. For instance, circRNA cSMARCA5 impaired HCC cell growth and migration through up-

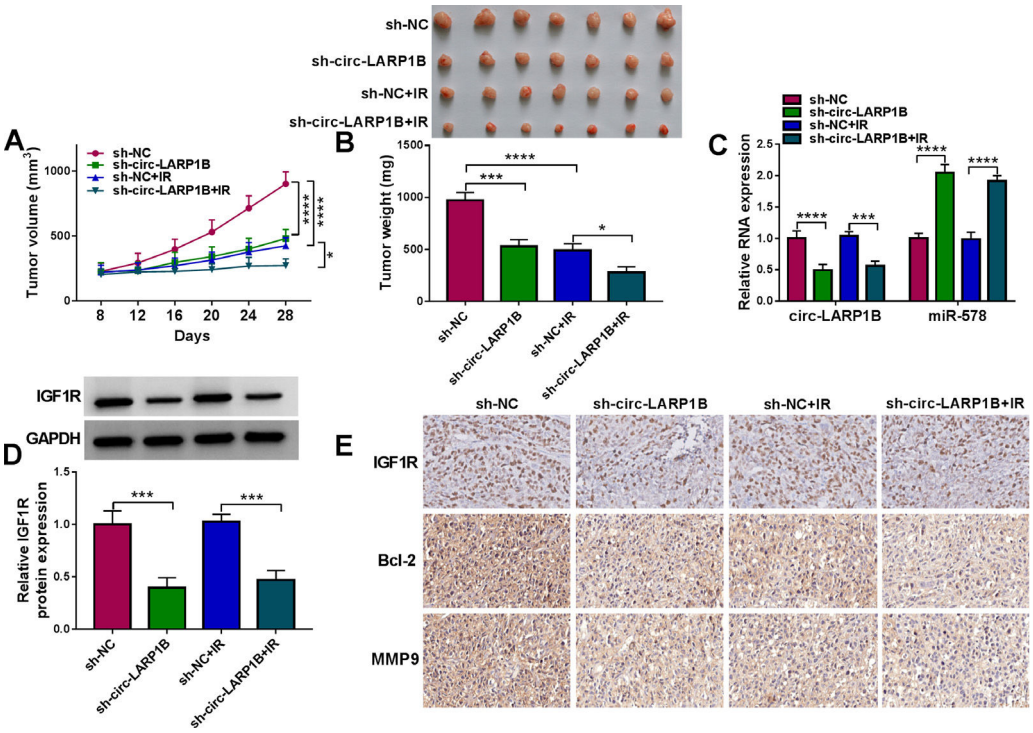

Fig. 8. Circ-LARP1B impedes tumor growth and enhances irradiation sensitivity in HCC *in vivo*. (A) Detection of tumor volume of each group was conducted every 4 days starting 8 days after inoculation. (B) Tumor weight of each group was detected at day 28 and the representative images of xenografts were shown. (C, D) qRT-PCR and Western blot analysis of circ-LARP1B, miR-578 and IGF1R expression levels in tumors isolated from each group. (E) Representative images of IGF1R, Bcl-2 and MMP9 protein staining in tumors of each group. $^{*}P < 0.05$, $^{***}P<0.001$, $^{****}P<0.0001$.

regulating TIMP3 by sequestering miR-181b-5p or miR-17-3p [10]. Wang's team showed that circRHOT1 targeted NR2F6 to contribute to HCC cell proliferation, migration and invasion [27]. Besides, circRNA-SORE was demonstrated to spread sorafenib resistance in HCC by biding to YBX1 [28]. In this study, circ-LARP1B as a conserved circRNA was found to be elevated in HCC patients, and highly expressed circ-LARP1B possessed poor outcome. Further functional experiments exhibited that knockdown of circ-LARP1B restrained HCC cell growth, invasion, angiogenesis, and enhanced cell radiosensitivity *in vitro*. Importantly, *in vivo* assay also suggested that circ-LARP1B silencing reduced tumor growth, invasion and expedited irradiation sensitivity in HCC. Thus, circ-LARP1B acts as an oncogene to regulate HCC progression and radiosensitivity.

CircRNAs located in the cytoplasm have been documented to serve as endogenous sponges of miRNAs to modulate the expression of their target genes [29,30]. In the current study, we confirmed that circ-LARP1B was preferentially localized in the cytoplasm in HCC cells. Therefore, the miRNA-mRNA axis underlying circ-LARP1B was identified, and this study verified that circ-LARP1B directly targeted miR-578 to block miR-578-mediated IGF1R degradation, the circ-LARP1B/miR-578/IGF1R axis was firstly investigated in HCC. MiR-578 is a functional miRNA, which was indicated to act as a target of circRNAs, such as circ_001621 and circZFR, to regulate the progression of osteosarcoma [31] or breast cancer [32]. In HCC, Wu et al. suggested that miR-578 was decreased and lowly expressed miR-578 was related to poor outcome, besides that, overexpression of miR-578 suppressed cancer cell growth and metastasis [33]. IGF1R is an important component of IGF system, which works on cell proliferation, adipogenesis, invasion, multidrug resistance and radioresistance [34–36]. Additionally, abnormal IGF1R expression has been identified in HCC, and silencing of IGF1R significantly repressed HCC tumor growth [37,38]. In the present work, we demonstrated that miR-578 suppressed HCC cell growth, invasion, angiogenesis, importantly, it also enhanced cell radiosensitivity, however, these effects were partially attenuated by IGF1R overexpression. Besides that, rescue assay implied that miR-578 inhibition abated the effects of circ-LARP1B knockdown on HCC cells.

In a word, we for the first time confirmed that circ-LARP1B was associated with poor prognosis of HCC patients, and circ-LARP1B upregulated IGF1R through miR-578 to promote HCC tumorigenicity and reduce radiosensitivity. Recently, knocking down or overexpressing circRNAs has been identified to be an important strategy to intervene cancer carcinogenesis, metastasis, and drug resistance [39]. Therefore, circ-LARP1B knockdown by siRNAs may a promising therapeutic strategy for HCC. Whereas how to achieve safe, efficient and target oriented delivery of siRNAs remains the major challenges in most siRNA therapeutics that need to overcome. The investigations on siRNA nanocarrier for siNRA delivery are future study directions. Besides that, there are still some limitations. New studies should be conducted to investigate the role of circ-LARP1B/miR-578/IGF1R axis in normal liver cells, thus illustrating the value of circ-LARP1B in clinical application for HCC treatment.

Conflicts of interest

The authors declare that they have no conflicts of interest.

Acknowledgement

None.

Funding

This study was supported by Clinical Research Fund Project of Zhejiang Medical Association (No.2019ZYC-A68).

Ethics approval and consent participate

All procedures were approved by the Institutional Animal Care and Use Committee of Lishui People's Hospital.

Consent for publication

Not applicable.

Availability of data and materials

Please contact the correspondence author for the data request.

References

[1] Llovet JM, Kelley RK, Villanueva A, Singal AG, Pikarsky E, Roayaie S, Lencioni R, Koike K, Zucman-Rossi J, Finn RS. Hepatocellular carcinoma. Nat Rev Dis Prim 2021;7(1):6.

[2] Fan ST, Poon RT, Yeung C, Lam CM, Lo CM, Yuen WK, Ng KK, Liu CL, Chan SC. Outcome after partial hepatectomy for hepatocellular cancer within the Milan criteria. Br J Surg 2011;98(9):1292–300.

[3] Yeung CSY, Chiang CL, Wong NSM, Ha SK, Tsang KS, Ho CHM, Wang B, Lee VWY, Chan MKH, Lee FAS. Palliative liver radiotherapy (RT) for symptomatic hepatocellular carcinoma (HCC). Sci Rep 2020;10(1):1254.

[4] Rizzo A, Ricci AD, Brandi G. Immune-based combinations for advanced hepatocellular carcinoma: shaping the direction of first-line therapy. Future Oncol 2021;17(7):755–7 (London, England).

[5] Rizzo A, Dadduzio V, Ricci AD, Massari F, Di Federico A, Gadaleta-Caldarola G, Brandi G. Lenvatinib plus pembrolizumab: the next frontier for the treatment of hepatocellular carcinoma? Expert Opin Investig Drugs 2021:1–8.

[6] Rizzo A, Brandi G. Biochemical predictors of response to immune checkpoint inhibitors in unresectable hepatocellular carcinoma. Cancer Treat Res Commun 2021;27:100328.

[7] Baskar R, Lee KA, Yeo R, Yeoh KW. Cancer and radiation therapy: current advances and future directions. Int J Med Sci 2012;9(3):193–9.

[8] Seong J, Park HC, Han KH, Lee DY, Lee JT, Chon CY, Moon YM, Suh CO. Local radiotherapy for unresectable hepatocellular carcinoma patients who failed with transcatheter arterial chemoembolization. Int J Radiat Oncol Biol Phys 2000;47(5):1331–5.

[9] Shiina S, Tateishi R, Arano T, Uchino K, Enooku K, Nakagawa H, Asaoka Y, Sato T, Masuzaki R, Kondo Y, et al. Radiofrequency ablation for hepatocellular carcinoma: 10-year outcome and prognostic factors. Am J Gastroenterol 2012;107(4):569–77 quiz 578.

[10] Yu J, Xu QG, Wang ZG, Yang Y, Zhang L, Ma JZ, Sun SH, Yang F, Zhou WP. Circular RNA cSMARCA5 inhibits growth and metastasis in hepatocellular carcinoma. J Hepatol 2018;68(6):1214–27.

[11] Barrett SP, Salzman J. Circular RNAs: analysis, expression and potential functions. Development 2016;143(11):1838–47.

[12] Chen B, Huang S. Circular RNA: An emerging non-coding RNA as a regulator and biomarker in cancer. Cancer Lett 2018;418:41–50.

[13] Chaichian S, Shafabakhsh R, Mirhashemi SM, Moazzami B, Asemi Z. Circular RNAs: a novel biomarker for cervical cancer. J Cell Physiol 2020;235(2):718–24.

[14] Zong L, Sun Q, Zhang H, Chen Z, Deng Y, Li D, Zhang L. Increased expression of circRNA_102231 in lung cancer and its clinical significance. Biomed Pharmacother 2018;102:639–44.

[15] Wu J, Qi X, Liu L, Hu X, Liu J, Yang J, Yang J, Lu L, Zhang Z, Ma S, et al. Emerging epigenetic regulation of circular RNAs in human cancer. Mol Ther Nucleic Acids 2019;16:589–96.

[16] Wang M, Ma M, Yang Y, Li C, Wang Y, Sun X, Wang M, Sun Y, Jiao W. Overexpression of hsa_circ_0008274 inhibited the progression of lung adenocarcinoma by regulating HMGA2 via sponging miR-578. Thorac Cancer 2021;12(16):2258–64.

[17] Chen RX, Liu HL, Yang LL, Kang FH, Xin LP, Huang LR, Guo QF, Wang YL. Circular RNA circRNA_0000285 promotes cervical cancer development by regulating FUS. Eur Rev Med Pharmacol Sci 2019;23(20):8771–8.

[18] An X, Liu X, Ma G, Li C. Upregulated circular RNA circ_0070934 facilitates cutaneous squamous cell carcinoma cell growth and invasion by sponging miR-1238 and miR-1247-5p. Biochem Biophys Res Commun 2019;513(2):380–5.

[19] Zhang DW, Wu HY, Zhu CR, Wu DD. CircRNA hsa_circ_0070934 functions as a competitive endogenous RNA to regulate HOXB7 expression by sponging miR-1236-3p in cutaneous squamous cell carcinoma. Int J Oncol 2020;57(2):478–87.

[20] Liang Y, Song X, Li Y, Chen B, Zhao W, Wang L, Zhang H, Liu Y, Han D, Zhang N, et al. LncRNA BCRT1 promotes breast cancer progression by targeting miR-1303/PTBP3 axis. Mol Cancer 2020;19(1):85.

[21] Bray F, Ferlay J, Soerjomataram I, Siegel RL, Torre LA, Jemal A. Global cancer statistics 2018: GLOBOCAN estimates of incidence and mortality worldwide for 36 cancers in 185 countries. CA Cancer J Clin 2018;68(6):394–424.

[22] Delaney G, Jacob S, Featherstone C, Barton M. The role of radiotherapy in cancer treatment: estimating optimal utilization from a review of evidence-based clinical guidelines. Cancer 2005;104(6):1129–37.

[23] Park SY, Lee CJ, Choi JH, Kim JH, Kim JW, Kim JY, Nam JS. The JAK2/STAT3/CCND2 Axis promotes colorectal Cancer stem cell persistence and radioresistance. J Exp Clin Cancer Res 2019;38(1):399.

[24] Roh MS, Colangelo LH, O'Connell MJ, Yothers G, Deutsch M, Allegra CJ, Kahlenberg MS, Baez-Diaz L, Ursiny CS, Petrelli NJ, et al. Preoperative multimodality therapy improves disease-free survival in patients with carcinoma of the rectum: NSABP R-03. J Clin Oncol 2009;27(31):5124–30.

[25] Cui C, Yang J, Li X, Liu D, Fu L, Wang X. Functions and mechanisms of circular RNAs in cancer radiotherapy and chemotherapy resistance. Mol Cancer 2020;19(1):58.

[26] Su M, Xiao Y, Ma J, Tang Y, Tian B, Zhang Y, Li X, Wu Z, Yang D, Zhou Y, et al. Circular RNAs in Cancer: emerging functions in hallmarks, stemness, resistance and roles as potential biomarkers. Mol Cancer 2019;18(1):90.

[27] Wang L, Long H, Zheng Q, Bo X, Xiao X, Li B. Circular RNA circRHOT1 promotes hepatocellular carcinoma progression by initiation of NR2F6 expression. Mol Cancer 2019;18(1):119.

[28] Xu J, Ji L, Liang Y, Wan Z, Zheng W, Song X, Gorshkov K, Sun Q, Lin H, Zheng X. CircRNA-SORE mediates sorafenib resistance in hepatocellular carcinoma by stabilizing YBX1. Signal Transduct Target Ther 2020;5(1):298.

[29] Hansen TB, Jensen TI, Clausen BH, Bramsen JB, Finsen B, Damgaard CK, Kjems J. Natural RNA circles function as efficient microRNA sponges. Nature 2013;495(7441):384–8.

[30] Thomson DW, Dinger ME. Endogenous microRNA sponges: evidence and controversy. Nat Rev Genet 2016;17(5):272–83.

[31] Ji X, Shan L, Shen P, He M. Circular RNA circ_001621 promotes osteosarcoma cells proliferation and migration by sponging miR-578 and regulating VEGF expression. Cell Death Dis 2020;11(1):18.

[32] Chen Z, Wang F, Xiong Y, Wang N, Gu Y, Qiu X. CircZFR functions as a sponge of miR-578 to promote breast cancer progression by regulating HIF1A expression. Cancer Cell Int 2020;20:400.

[33] Wu A, Li Y, Kong M, Zhu B, Liu R, Bao F, Ju S, Chen L, Wang F. Upregulated hsa_circ_0005785 facilitates cell growth and metastasis of hepatocellular carcinoma through the miR-578/APRIL axis. Front Oncol 2020;10:1388.

[34] Tseng YH, Kokkotou E, Schulz TJ, Huang TL, Winnay JN, Taniguchi CM, Tran TT, Suzuki R, Espinoza DO, Yamamoto Y, et al. New role of bone morphogenetic protein 7 in brown adipogenesis and energy expenditure. Nature 2008;454(7207):1000–4.

[35] Samani AA, Yakar S, LeRoith D, Brodt P. The role of the IGF system in cancer growth and metastasis: overview and recent insights. Endocr Rev 2007;28(1):20–47.

[36] Guvakova MA. Insulin-like growth factors control cell migration in health and disease. Int J Biochem Cell Biol 2007;39(5):890–909.

[37] Yao M, Wang L, Yang J, Yan X, Cai Y, Yao D. IGF-I receptor as an emerging potential molecular-targeted for hepatocellular carcinoma *in vitro* and *in vivo*. Tumour Biol 2016;37(11):14677–86.

[38] Wang L, Yao M, Zheng W, Fang M, Wu M, Sun J, Dong Z, Yao D. Insulin-like growth factor i receptor: a novel target for hepatocellular carcinoma gene therapy. Mini Rev Med Chem 2019;19(4):272–80.

[39] Zhang Y, Wang Y, Su X, Wang P, Lin W. The value of circulating circular RNA in cancer diagnosis, monitoring, prognosis, and guiding treatment. Front Oncol 2021;11:736546.